Materials Technology Reports 2024, 2(1), 483.
https://doi.org/10.59400/mtr.v2i1.483

Article

Electrochemical performance of $Pr_{0.6}Sr_{0.4}Fe_{0.8}Co_{0.2}O_{3-\delta}$ as potential cathode material for IT-SOFC

M. Shamshi Hassan

Department of Chemistry, College of Science, Al-Baha University, Albaha 65799, Saudi Arabia; mshasan@bu.edu.sa

CITATION

Hassan MS. Electrochemical performance of $Pr_{0.6}Sr_{0.4}Fe_{0.8}Co_{0.2}O_{3-\delta}$ as potential cathode material for IT-SOFC. Materials Technology Reports. 2024; 2(1): 483. https://doi.org/10.59400/mtr.v2i1.483

ARTICLE INFO

Received: 3 November 2023
Accepted: 12 January 2024
Available online: 29 February 2024

Abstract: Solid oxide fuel cells (SOFCs) are renowned for being effective energy sources that have potential to influence how energy is developed in future. SOFCs operate at low temperatures provides different benefits for widespread commercialization. In the present study a perovskite material $Pr_{0.6}Sr_{0.4}Fe_{0.8}Co_{0.2}O_{3-\delta}$ (PSFCo) was investigated as cathode for SOFC in intermediate temperature range. Glycine nitrate process was used for the preparation of the samples. PSFCo exhibited cubic structure having small particle size (100–200 nm). The electrical conductivity of the PSFCo was measured as function of temperature up to 850 ℃. The sample displayed maximum electrical conductivity of 370 Scm^{-1} at around 550–600 ℃. The polarization behavior of PSFCo was calculated by means of AC impedance with $Sm_{0.8}Ce_{0.2}O_2$ (SDC) as electrolyte. The value of area specific resistance (ASR) was calculated as 0.146 Ωcm^2 at 800 ℃ and 0.248 Ωcm^2 at 700 ℃.

Keywords: cathode; PSFCo; electrical conductivity; impedance spectra; IT-SOFC

1. Introduction

The urgent need to minimize carbon emissions on a global scale and the quick depletion of fossil fuel supplies are driving up predicted demand for renewable energy sources. Fuel cells are energy-conversion systems that electrochemically combine fuel and oxidant to generate electricity and heat without the Carnot constraint [1–3]. Comparatively, SOFCs provide a variety of fuel sources, minimal noise, low CO_2 emissions, a long lifespan (40,000–80,000 h), and excellent conversion rate [4,5].

Typical SOFCs run at temperatures of about 1000 ℃. However, the high temperature causes a lot of issues, for example, the materials get damaged because of chemical and physical instability. Thus, there is a rather narrow options for the components that can be utilized in the construction and subsequent operation of SOFCs. If the working temperature were decreased, the affordable ferritic stainless steel can be utilized as connector, and the components' chemical, thermal, and physical durability would all be improved too [6]. For the effective launch of SOFC technology to the market, reduced temperature operation at 600–800 ℃ is an essential factor. These reduced temperature SOFC offer shorter start-up times, are more readily realistically designed, and are economically preferable. One of the vital challenge for low temperature operation is to nullify the stability problems while keeping a positive efficiency. Nevertheless, the electrolytes' ion conductivity will drop and the cathode resistance will rise at such a low operating temperature. Hence, ceria-based electrolyte, like gadolinia-doped ceria (GDC) or samarium-doped ceria (SDC), is normally used due to its improved ionic conductivity in decreased temperature range than yttria stabilized zirconia (YSZ) which is commonly utilized as electrolyte for high temperature SOFCs. But a significant problem with the lower operating temperature

is that the cathode's catalytic activity for oxygen reduction will decreased [7]. Thereby, it is crucial to find substitute materials, like perovskite cathodes, in order to guarantee the extremely stable and dependable operation of the resulting SOFCs, as well as practically acceptable performance. During past years adequate research investigation performed to ascertain appropriate material as cathode for application in SOFC that can work at intermediate temperature (500–800 ℃). Though, the electrode activity significantly declines as the operating temperature is lowered. The creation of high-performance cathode materials is essential for further enhancing fuel cell performance. Cathode is a significant part of the fuel cell which effectively determines the overall fuel cells performance. Among high performing cathodes, ABO_3 types are one of the best. The perovskite configuration (ABO_3) can be altered by exchanging A or B position positive ion by other elements. Praseodymium is one of the materials being utilized on A-site. The structural and electronic configuration of praseodymium resembles with other lanthanide elements like cerium and lanthanum [8]. Substituting lanthanum with smaller lanthanide has been reported to show better performance as cathode material [9,10]. Previous reports have shown that the exchange of La by Pr improves the conductivity and catalytic activity [11–13]. Strontium doped praseodymium cobaltite or manganites have been stated to show excellent electrical, ionic conductivity and overpotential values [14–20]. Doping cobalt by substituting iron on B-site of the ABO_3 type have been shown to exhibit effective performance as cathode material [21–24].

In this study, a new type of perovskite oxide was developed for the cathode of IT-SOFCs by doping Sr at the A site and Co at the B site of the $PrFeO_{3-\delta}$-based perovskite material. Even after doping of the elements on A and B-site in compound, it did not change its cubic structure and it remain stable even at high temperature without any impurity. The cathode materials are designed to improve the cathode performance at intermediate temperatures. PSFCo has shown promising electrical properties and low value of area specific resistance at IT-SOFCs.

2. Experimental

$Pr_{0.6}Sr_{0.4}Fe_{0.8}Co_{0.2}O_3$ powder was synthesized by glycine nitrate method reported elsewhere [25]. Analytical grade $Pr(NO_3)_3.6H_2O$ (Alfa Aesar, 99.9%), $Sr(NO_3)_2$ (Aldrich, 99%), $Fe(NO_3)_3.9H_2O$ (Samchun chemicals, 98.5%) and $Co(NO_3)_2.6H_2O$ (Alfa Aesar, 98%) were used. Glycine was used as oxidizer and fuel. The stoichiometric amounts of all the metal nitrates were mixed with DW (250 mL) in beaker. After dissolution, double mole of glycine (compare to metal nitrate) was added in the same solution. Solution was kept stirring and the hot plate temperature were increased to 200 ℃. Gradually, the viscosity of the solution increases with times which lead to combustion reaction leaving dark grey ash in beaker. The sample was collected and heated at different temperature under air to burn off carbon. The sample powder was hard-pressed into pallet and calcined at 1200 ℃ for 5 h.

To determine the crystallinity of synthesized material, X-ray diffraction (XRD, Rigaku) study was performed by Rigaku D/Max diffractometer with Cu Kα radiation. Chemical composition of PSFCo was observed by Energy Dispersive X-ray (EDX, JEOL JSM6700) spectroscopy. The study of microstructures of synthesized samples

was executed by Scanning Electron Microscopy (SEM, JEOL JSM6700) and Transmission Electron Microscopy (TEM, Hitachi H-7650). Electrical conductivity of the PSFeCo material was calculated using the standard 4 probe DC method. The $Ce_{0.8}Sm_{0.2}O_2$ (SDC) electrolyte sample was also synthesized by the same glycine nitrate method. This electrolyte powder was pressed into round pallets (15 mm in diameter) and calcined at 1450 ℃ for 5 h in furnace. The electrochemical properties and AC impedance were measured by impedance analyzer (VersaSTAT 4).

3. Result and discussion

The X-ray pattern of the PSFCo samples is shown in **Figure 1a** calcined at various temperatures. XRD results showed a single-phased powder with perovskite-type cubic structure (Pm-3m space group) similar to that of $Pr_{1-x}Sr_xFeO_3$, is formed [26]. As the temperature increases, the spectral peaks became sharper showing higher crystallinity without detectable impurity phases. EDX result of prepared PSFCo material was shown in **Figure 1b**. From the attained EDX outcomes, it is obvious that the produced $Pr_{0.6}Sr_{0.4}Fe_{0.8}Co_{0.2}O_{3-\delta}$ material contains only Pr, Sr, Fe, Co and O elements with no contamination. **Figure 1c,d** depicts the SEM image PSFCo cathode synthesized at 1000 ℃ and cross-section view of PSFCo/SDC interface. The microstructure looks to be consistent with well necked granules and high porosity (**Figure 1c**). The electrode microstructure showed uniform and uneven attachment with electrolyte. The coating of PSFCo cathode on 1mm thick SDC electrolyte seems to be intact. The electrolyte layers exhibit compressed micro-structure devoid of cracks and pinholes. The thickness of electrode on electrolyte is about 35 μm (**Figure 1d**).

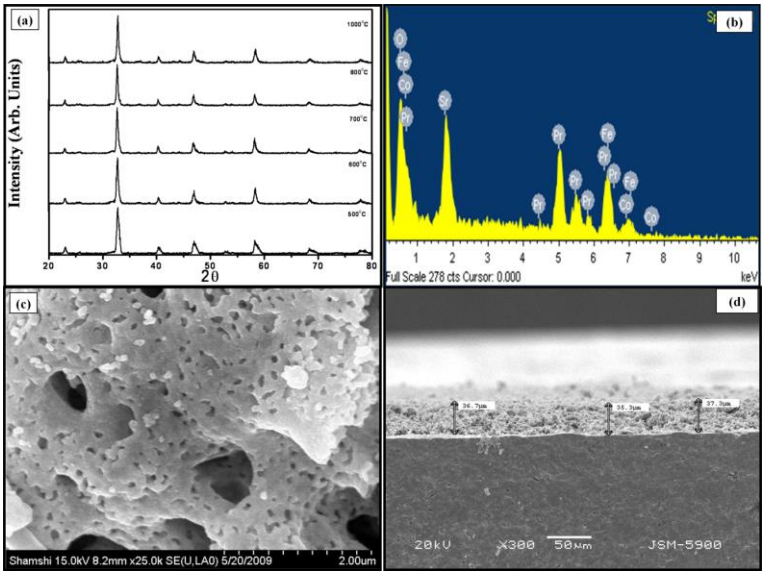

Figure 1. (a) the XRD spectra of the $Pr_{0.6}Sr_{0.4}Fe_{0.8}Co_{0.2}O_{3-\delta}$ samples at 500, 600, 700, 800 and 1000 ℃; **(b)** EDX spectrum; **(c)** SEM images of $Pr_{0.6}Sr_{0.4}Fe_{0.8}Co_{0.2}O_{3-\delta}$ powder synthesized at 1000 ℃; and **(d)** cross-section view of SDC-PSFCo interface.

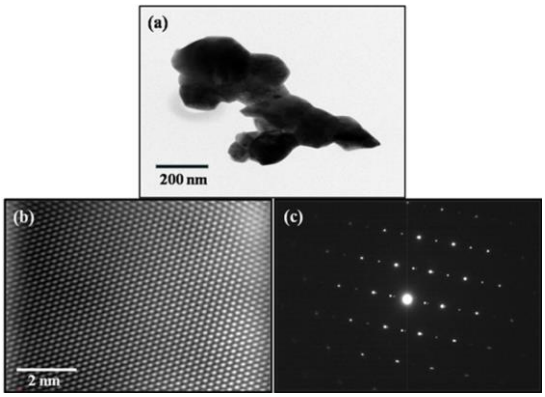

Figure 2. (a) TEM; **(b)** HR-TEM; and **(c)** SAED pattern of $Pr_{0.6}Sr_{0.4}Fe_{0.8}Co_{0.2}O_{3-\delta}$ particle.

Figure 2a,b demonstrates the TEM and HRTEM of the primed material whereas **Figure 2c** characterize the selected area electron diffraction pattern (SAED). The TEM result showed the agglomerated particles showing size in between 100 to 200 nm. HR-TEM reveals the high crystallinity of the material, the atomic planes are parallel and have regular arrangement of atoms. Additionally, the SAED pattern reveals high standard of crystallinity. Lattice planes have no disorders or defects revealing high crystallinity of material.

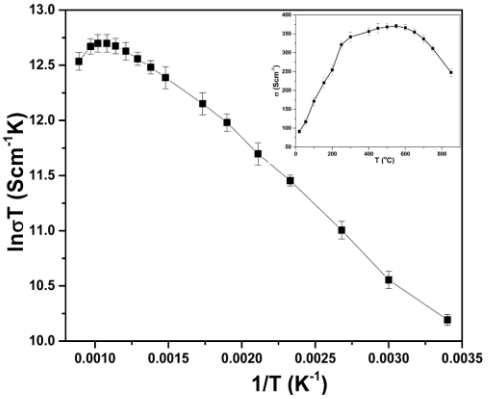

Figure 3. Arrhenius plot of DC conductivity (lnσT) vs. 1/T. Inset shows the electrical conductivity for $Pr_{0.6}Sr_{0.4}Fe_{0.8}Co_{0.2}O_{3-\delta}$. pallet measured from room temperature to 850 ℃.

Electrical conductivity of the cathode pellet was measured as function of inverse temperature in **Figure 3**. The simultaneous presence of oxygen vacancies and electron holes in perovskite-type materials results in both ionic and electronic conductivities; nevertheless, the ionic conductivity of the material is far less than the electronic conductivity. Synthesized sample showed the semiconducting behavior, as the electrical conductivity increase with increase in temperature through a maximum, then declined at elevated temperature representing that a dissimilar mechanism of conduction takes place at diverse temperature. The sample displayed maximum conductivity of 370 Scm^{-1} at around 550–600 and it remain more than 200 Scm^{-1} even at 850 ℃ (**Figure 3**). After linear fitting from graph, the estimate of activation energy was calculated as 8.6 $KJmol^{-1}$. The high value of conductivity is owing to the increase

in concentration of B^{+4} cations (Fe^{+4}or Co^{+4}). The conductivity decrease at high temperature can be ascribe to appearance of oxygen vacancies along with reduction of B^{+4} to B^{+3} (Fe^{+3} or Co^{+3}) which leads to decrease in charge carrier concentration. Furthermore, a reduction in iron ions impacts the electron transport between Fe–O–Fe bonds, resulting in a decline in electronic conductivity. This decline has the greatest influence on the total electrical conductivity [27].

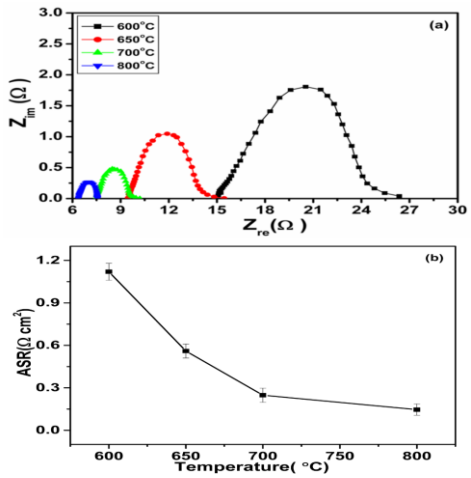

Figure 4. (a) impedance spectra for $Pr_{0.6}Sr_{0.4}Fe_{0.8}Co_{0.2}O_{3-\delta}$ cathode in air at various temperature; **(b)** area specific resistance (ASR) of the PSFC measured at different temperature.

The typical impedance for symmetrical cells PSFCo/SDC/PSFCo at various temperatures (600, 650, 700 and 800 °C) are revealed in **Figure 4**. Herein, it is noticed that electrode polarization resistance (P_R) of PSFCo cathode on SDC electrolyte increased with temperature (**Figure 4a**). This phenomena possibly attributed to increase in number of oxygen ion vacancy on the cathode surface which helps in oxygen molecule $O_{2(ad)}$ dissociation to oxygen atom $O_{(ad)}$ [28]. The value of ASR (Ωcm^2) as a parameter of temperature for PSFCo cathode in air is shown in inset in **Figure 4b**. The ASR decreases as temperature increases from 1.21 Ωcm^2 at 600 °C, 0.56 Ωcm^2 at 650 °C, 0.248 Ωcm^2 at 700 °C to 0.146 Ωcm^2 at 800 °C. ASR signifies the overall cathodic features assigned to oxygen reduction, oxygen surface/bulk diffusion and gas-phase oxygen diffusion [29]. This indicates that PSFCo cathode has elevated electrocatalytic performance for oxygen reduction reactions at reduced temperatures. Thus, we can say that PSFCo cathode can be a promising and good material for application in IT-SOFC.

4. Conclusion

$Pr_{0.6}Sr_{0.4}Fe_{0.8}Co_{0.2}O_{3-\delta}$ cathode was successfully prepared by glycine nitrate method and characterized by physico-chemical properties. It's electrical and electrochemical properties was also investigated for potential usage as cathode material for IT-SOFC. The sample features cubic structure with 100–200 nm sized particle. XRD results showed a single-phased powder with perovskite-type cubic structure. The sample displayed the semiconductor to metal conduction transition with maximum conductivity of 370 Scm^{-1} at around 550–600 °C. Therefore, they may be

use as a potential cathode in IT-SOFC. The ASR value of symmetrical PSFC cathode in air were 1.21 Ωcm^2, 0.56 Ωcm^2, 0.248 Ωcm^2 and 0.146 Ωcm^2 at 600 ℃, 650 ℃, 700 ℃ and 800 ℃ respectively. The PSFCo cathode has demonstrated promising catalytic activity for oxygen reduction. Hence, we can conclude that PSFCo can be a cheap, efficient, stable, and promising material to use as cathode at intermediate temperature in SOFC. Further investigation is required to evaluate the long-term stability and chemical compatibility on this material.

Conflict of interest: The author declares no conflict of interest.

References

1. Richter J, Holtappels P, Graule T, et al. Materials design for perovskite SOFC cathodes. Monatshefte für Chemie—Chemical Monthly. 2009; 140(9): 985-999. doi: 10.1007/s00706-009-0153-3
2. Choudhury R, Das UJ, Ceruti A, et al. Visco-elastic effects on the three dimensional hydrodynamic flow past a vertical porous plate. Int. Inf. Eng. Technol. Assoc. 2013; 31: 1-8.
3. Ashrafi H, Pourmahmoud N, Mirzaee I, et al. Performance improvement of proton-exchange membrane fuel cells through different gas injection channel geometries. International Journal of Energy Research. 2022; 46(7): 8781-8792. doi: 10.1002/er.7755
4. Gao Y, Zhang M, Fu M, et al. A comprehensive review of recent progresses in cathode materials for Proton-conducting SOFCs. Energy Reviews. 2023; 2(3): 100038. doi: 10.1016/j.enrev.2023.100038
5. Cigolotti V, Genovese M, Fragiacomo P. Comprehensive Review on Fuel Cell Technology for Stationary Applications as Sustainable and Efficient Poly-Generation Energy Systems. Energies. 2021; 14(16): 4963. doi: 10.3390/en14164963
6. Li H, Wang Y, Liu H, et al. Interaction between SOFCs interconnect Cr-free multicomponent spinel coating materials and chromia. International Journal of Hydrogen Energy. 2023; 48(81): 31700-31707. doi: 10.1016/j.ijhydene.2023.04.324
7. Colomer MT, Steele BCH, Kilner JA. Structural and electrochemical properties of the $Sr_{0.8}Ce_{0.1}Fe_{0.7}Co_{0.3}O_{3-\delta}$ perovskite as cathode material for ITSOFCs. Solid State Ionics. 2002; 147(1-2): 41-48.
8. Ran R, Wu X, Quan C, et al. Effect of strontium and cerium doping on the structural and catalytic properties of PrMnO oxides. Solid State Ionics. 2005; 176(9-10): 965-971. doi: 10.1016/j.ssi.2004.11.018
9. Riza F, Ftikos C, Tietz F, Fischer W. Preparation and Characterization of $Ln_{0.8}Sr_{0.2}Fe_{0.8}Co_{0.2}O_3$−x(Ln= La, Pr, Nd, Sm, Eu, Gd). Journal of the European Ceramic Society. 2001; 21: 1769-1773.
10. Qiu L, Ichikawa T, Hirano A, et al. Ln1−xSrxCo1−yFeyO3−δ (Ln = Pr, Nd, Gd; x = 0.2, 0.3) for the electrodes of solid oxide fuel cells. Solid State Ionics. 2003; 158: 55-65.
11. Ishihara T, Kudo T, Matsuda H, et al. Doped PrMnO3 Perovskite Oxide as a New Cathode of Solid Oxide Fuel Cells for Low Temperature Operation. Journal of The Electrochemical Society. 1995; 142(5): 1519-1524. doi: 10.1149/1.2048606
12. Ishihara T, Honda M, Shibayama T, et al. Intermediate Temperature Solid Oxide Fuel Cells Using a New LaGaO3 Based Oxide Ion Conductor: I. Doped as a New Cathode Material. Journal of The Electrochemical Society. 1998; 145(9): 3177-3183. doi: 10.1149/1.1838783
13. Kostogloudis GC, Vasilakos N, Ftikos C. Crystal structure, thermal and electrical properties of Pr1−xSrxCoO3−δ (x = 0, 0.15, 0.3, 0.4, 0.5) perovskite oxides. Solid State Ionics. 1998; 106: 207-218.
14. Steele BC, Bae JM. Properties of $La_{0.6}Sr_{0.4}Co_{0.2}Fe_{0.8}O_{3-x}$ (LSCF) double layer cathodes on gadolinium-doped cerium oxide (CGO) electrolytes: II. Role of oxygen exchange and diffusion. Solid State Ionics. 1998; 106: 255-261.
15. Xia C, Rauch W, Chen F, Liu M. $Sm_{0.5}Sr_{0.5}CoO_3$ cathodes for low-temperature SOFCs. Solid State Ionics. 2002; 149: 11-19.
16. Al Daroukh M, Vashook V, Ullmann H, et al. Oxides of the AMO3 and A2MO4-type: structural stability, electrical conductivity and thermal expansion. Solid State Ionics. 2003; 158: 141-150.
17. Wang Y, Wang S, Wang Z, et al. Performance of Ba0.5Sr0.5Co0.8Fe0.2O3−δ-CGO-Ag cathode for IT-SOFCs. Journal of Alloys and Compounds. 2007; 428(1-2): 286-289. doi: 10.1016/j.jallcom.2006.02.071
18. Chen W, Wen T, Nie H, Zheng R. Study of Ln0.6Sr0.4Co0.8Mn0.2O3-δ (Ln = La, Gd, Sm or Nd) as the cathode materials for intermediate temperature SOFC. Materials research bulletin. 2003; 38: 1319-1328.
19. Rossignol C, Ralph J, Bae JM, Vaughey J. Ln1−xSrxCoO3 (Ln = Gd, Pr) as a cathode for intermediate-temperature solid

oxide fuel cells. Solid State Ionics. 2004; 175: 59-61.
20. Kim JH, Baek SW, Lee C, et al. Performance analysis of cobalt-based cathode materials for solid oxide fuel cell. Solid State Ionics. 2008; 179(27-32): 1490-1496. doi: 10.1016/j.ssi.2008.01.086
21. Tai LW, Nasrallah M, Anderson H, et al. Structure and electrical properties of La1−xSrxCo1−yFeyO3. Part 1. The system La0.8Sr0.2Co1−yFeyO3. Solid State Ionics. 1995; 76: 259-271.
22. Chen X, Wu N, Ignatiev A. Structure and conducting properties of La1-xSrxCoO3-δ films. Journal of the European Ceramic Society. 1999; 19: 819-822. doi: 10.1016/S0955-2219(98)00323-9
23. Chen X, Wu NJ, Smith L, et al. Thin-film heterostructure solid oxide fuel cells. Applied Physics Letters. 2004; 84(14): 2700-2702. doi: 10.1063/1.1697623
24. Pederson LR, Singh P, Zhou XD. Application of vacuum deposition methods to solid oxide fuel cells. Vacuum. 2006; 80(10): 1066-1083. doi: 10.1016/j.vacuum.2006.01.072
25. Zamani F, Taghvaei AH. Characterization and magnetic properties of nanocrystalline Mg1-CdFe2O4 (x= 0.0–0.8) ferrites synthesized by glycine-nitrate autocombustion method. Ceramics International. 2018; 44(14): 17209-17217. doi: 10.1016/j.ceramint.2018.06.178
26. Piao J, Sun K, Zhang N, et al. Preparation and characterization of Pr1−xSrxFeO3 cathode material for intermediate temperature solid oxide fuel cells. Journal of Power Sources. 2007; 172(2): 633-640. doi: 10.1016/j.jpowsour.2007.05.023
27. Gou Y, Li G, Ren R, et al. Pr-Doping Motivating the Phase Transformation of the BaFeO3-δ Perovskite as a High-Performance Solid Oxide Fuel Cell Cathode. ACS Applied Materials & Interfaces. 2021; 13(17): 20174-20184. doi: 10.1021/acsami.1c03514
28. Steele BC. Survey of materials selection for ceramic fuel cells II. Cathodes and anodes. Solid State Ionics. 1996; 86: 1223-1234.
29. Aysal HE, Kılıç F, Çakmak G, et al. Thermal plasma synthesis of (La,Sr)CoO3-(La,Sr)2CoO4 composite cathodes for intermediate temperature solid oxide fuel cells (IT-SOFC). International Journal of Hydrogen Energy. 2024; 51: 1477-1486. doi: 10.1016/j.ijhydene.2023.07.031